



## ARTICLE

# A Novel Transcatheter Suture Closure System for Patent Foramen Ovale: An Experimental Study in Swine

Su Ye<sup>1</sup>, Luxi Guan<sup>1</sup>, Dong Luo<sup>1</sup>, Fengwen Zhang<sup>1</sup>, Jianhua Lv<sup>1</sup>, Qizong Xie<sup>2</sup>, Qiao Huang<sup>2</sup>, Haiming Wu<sup>2</sup>, Haibo Hu<sup>1,\*</sup> and Xiangbing Pan<sup>1,\*</sup>

<sup>1</sup>Center of Structural Heart Disease, State Key Laboratory of Cardiovascular Disease, Fuwai Hospital, National Center for Cardiovascular Diseases, Chinese Academy of Medical Sciences and Peking Union Medical College, Beijing, 100037, China

<sup>2</sup>Halocinch Medical Technology (Shenzhen) Co., Ltd., Yifenghua Innovation Industrial Park, Dalang Street, Longhua District, Shenzhen, 518109, China

\*Corresponding Authors: Haibo Hu. Email: hhb.fwhospital@hotmail.com; Xiangbing Pan. Email: panxiangbin@fuwaihospital.org

Received: 10 January 2025; Accepted: 22 April 2025; Published: 30 April 2025

**ABSTRACT: Objectives:** This study aimed to evaluate the feasibility, safety, and efficacy of a novel transcatheter suture closure system (HaloStitch<sup>®</sup>) for patent foramen ovale (PFO) closure in a swine model. **Methods:** Thirteen swine underwent experimental PFO model creation. All animals received implantation of the transcatheter suture closure system to evaluate procedural success. Comprehensive follow-up over six months included serial ultrasound imaging, histopathological analysis, and gross anatomical examination of cardiac specimens. **Results:** Successful HaloStitch<sup>®</sup> device implantation was achieved in 11 of 13 swine. Gross anatomical examination confirmed secure positioning of all sutures in the atrial septum, with no redundancy or thrombus formation. Postoperative ultrasound demonstrated stable suture and staple positions throughout follow-up, with no evidence of suture breakage, displacement, or thrombus. Staples were clearly visualized under ultrasound imaging. Both the atrial septal defect orifice diameter and residual septal shunt flow velocity decreased significantly during the observation period. Histopathological analysis revealed partially organized thrombi at the implant head and fibrous connective tissue encapsulation with localized inflammatory cell infiltration surrounding the polymer material. **Conclusions:** The transcatheter suture closure system (HaloStitch<sup>®</sup>) demonstrated feasibility, safety, and biocompatibility for PFO closure in a swine model, supporting its potential for clinical translation.

**KEYWORDS:** Patent foramen ovale; transcatheter suture closure system; experimental study

## 1 Introduction

The foramen ovale serves as a critical physiological passage in channel circulation, enabling blood from the umbilical vein to bypass the pulmonary circuit via the right-to-left atrial shunt. Postnatally, the foramen ovale typically closes spontaneously following the initiation of pulmonary circulation. Permanent closure, mediated by fibrous adhesion, occurs in approximately 25% of infants by one year of age. Persistence of this atrial communication beyond three years is clinically defined as a patent foramen ovale (PFO) [1].

Under physiological conditions, higher left atrial pressure ensures PFO valve closure, preventing hemodynamic abnormalities. However, elevated right atrial pressure may reopen



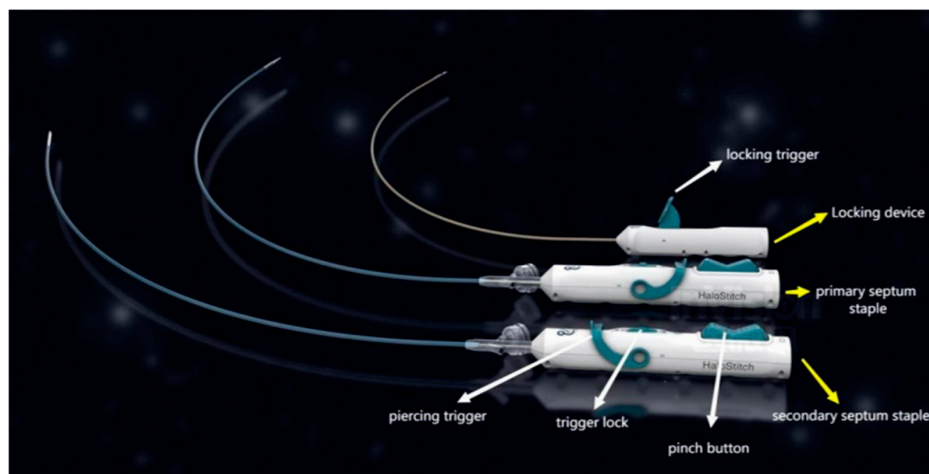
the valve, facilitating a right-to-left shunt and paradoxical embolism. PFO is implicated in diverse pathologies, including cryptogenic stroke, transient ischemic attacks, migraines, decompression sickness, platypnea-orthodeoxia syndrome, and high-altitude illness [2,3]. For patients with symptomatic PFO, transcatheter intervention has emerged as the preferred therapeutic approach, replacing traditional surgical and pharmacological strategies. Current occluders are broadly classified into non-degradable (e.g., Amplatzer and its derivatives) and biodegradable (e.g., IrisFIT and Chinese Lantern occluders) categories, based on material composition and structural design.

In this study, we evaluated the HaloStitch<sup>®</sup> transcatheter suture closure system (Halocinch Medical Technology, Shenzhen, China) in a healthy swine model. Our objectives were to assess the system's operational feasibility, safety profile, and efficacy, thereby providing foundational data to guide its clinical translation.

## 2 Methods

### 2.1 Equipment Composition and Principle

The transcatheter suture closure system for PFO comprises two primary components: the guide sheath system and the suture delivery system. The device establishes an access channel via femoral vein puncture. The suture system is advanced through the guide sheath into the right atrium, where its distal assembly engages and sutures the septum primum and septum secundum. Two sets of non-absorbable sutures are threaded through the septal tissues, followed by deployment of a locking device via the guide sheath. The locking mechanism secures the sutures to achieve complete PFO closure, after which excess suture material is trimmed. Fig. 1A illustrates the staples and locking device applied to the septum primum and secundum, Fig. 1B outlines the procedural steps of the suturing operation, and Fig. 1C explicitly details the critical deployment steps of the HaloStitch<sup>®</sup> system.



(A)

Figure 1: Cont.

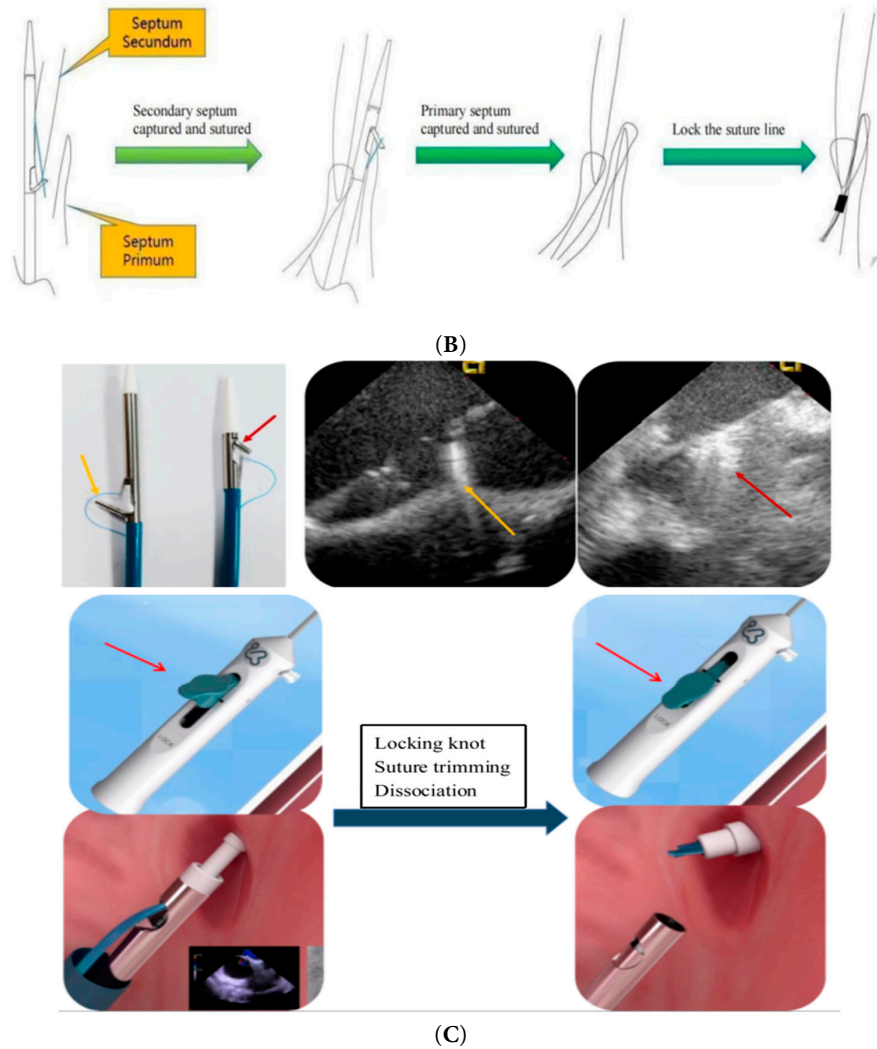


**Figure 1:** (A): Suture device appearance. (B): Sewing operation diagram. (C): Device positioning, Suture tightening.

## 2.2 Experimental Animals

The study included 13 swine (sex-unrestricted, weight range: 85–105 kg) from Experimental Animal Center, Fuwai Hospital, Beijing, China. All of the experiments were performed according to the guidelines of the Animal Care and Use Committee, Experimental Animal Center, Fuwai Hospital, National Center for Cardiovascular Diseases, China. Swine hearts exhibit high anatomical similarity to human hearts in terms of size, valve morphology, and coronary artery orientation, making them an optimal model for this research [4–8].

## 2.3 Preoperative Preparation

Three days prior to the procedure, the animals received daily oral administration of 75 mg clopidogrel and 100 mg aspirin. To ensure fasting conditions, food and water were withheld for 12 h preoperatively. During the procedure, general anesthesia was induced and maintained via inhalation. Vital parameters (hemodynamics, electrocardiography [ECG], and blood oxygen saturation) were continuously monitored. Auricular venous access was established for fluid

resuscitation and medication delivery. Transthoracic echocardiography (TTE) was performed to assess cardiac structure and function. Three blood samples were collected preoperatively via the anterior vena cava or vascular sheath for complete blood count, biochemistry, coagulation profile, and hemolysis analysis. Systemic heparinization was administered to maintain an activated clotting time (ACT) >300 s throughout implantation.

## **2.4 Animal Procedure**

### *2.4.1 Animal Model Creation and Establishing Vascular Access*

The left femoral vein was punctured to establish access for intracardiac ultrasound, while the left femoral artery was punctured for invasive blood pressure monitoring. The right femoral vein was accessed for atrial septal puncture and delivery of the PFO suture system. A guidewire was advanced from the right femoral venous sheath into the inferior vena cava and exteriorized through a 7F venous sheath. The atrial septal puncture sheath was exchanged over the guidewire, advanced through the superior vena cava into the right atrium, and the guidewire was subsequently withdrawn. An atrial septal puncture needle (tip positioned 0.5 mm inside the sheath) was advanced through the sheath, with its tail connected to a contrast-filled syringe. Under intracardiac ultrasound guidance, the needle punctured the fossa ovalis, and contrast injection confirmed entry into the left atrium (linear contrast spray), establishing the PFO model. Fig. 2A–E illustrates the stapler implantation under digital subtraction angiography (DSA) fluoroscopy.

Under combined ultrasound and X-ray guidance, the atrial septum was punctured, and a 0.035-inch guidewire was inserted into the pulmonary vein. The guide sheath system was advanced into the right atrium along the guidewire, followed by dilator removal.

### *2.4.2 Suture Device Operation*

The secundum septum suture device was advanced along the guidewire into the guide sheath until its distal end reached the superior vena cava. The guide sheath was slightly retracted to deploy the device arms, which were precisely positioned around the secundum septum. The arms were opened to engage and suture the secundum septum.

Subsequently, the primum septum suture device was advanced along the guidewire through the foramen ovale into the left atrium. The arms were opened to engage and suture the primum septum.

Finally, the locking device was then advanced along the suture lines to the right atrium. All four sutures were tightened to achieve complete closure, and the locking mechanism was activated to secure the sutures. Redundant suture material was trimmed using the built-in cutting feature.

### *2.4.3 Postoperative Echocardiography*

Following device removal, cardiac function indices, atrial septal defect size, and residual shunt velocity were assessed using intracardiac echocardiography (ICE), transthoracic echocardiography (TTE), and transesophageal echocardiography (TEE). Agitated saline contrast was injected into the femoral vein to evaluate right-to-left atrial shunting via echocardiography.

### 2.5 Postoperative Treatment and Follow-Up

In the week following the procedure, the animals received antibiotic prophylaxis comprising intramuscular ceftriaxone sodium (3.0 g twice daily). Additionally, wounds were disinfected twice daily using iodophor solution. A daily regimen of 100 mg aspirin and 75 mg clopidogrel was maintained until scheduled observation endpoints. Follow-up assessments were conducted at 1, 3, and 6 months postoperatively. Throughout this period, trained veterinary staff monitored the animals, documenting behavioral and physiological parameters such as activity levels, dietary intake, sleep patterns, respiratory status, and body temperature. Blood samples were collected preoperatively, immediately postoperatively, and at 1, 3, and 6 months postoperatively for complete blood count, biochemical profiling, coagulation testing, and hemolysis analysis. Serial ultrasonography was performed during follow-up appointments to evaluate postoperative outcomes.

At the conclusion of the observation period, the animals were humanely euthanized. Comprehensive post-mortem examinations, including gross anatomical and histological analyses, were performed.

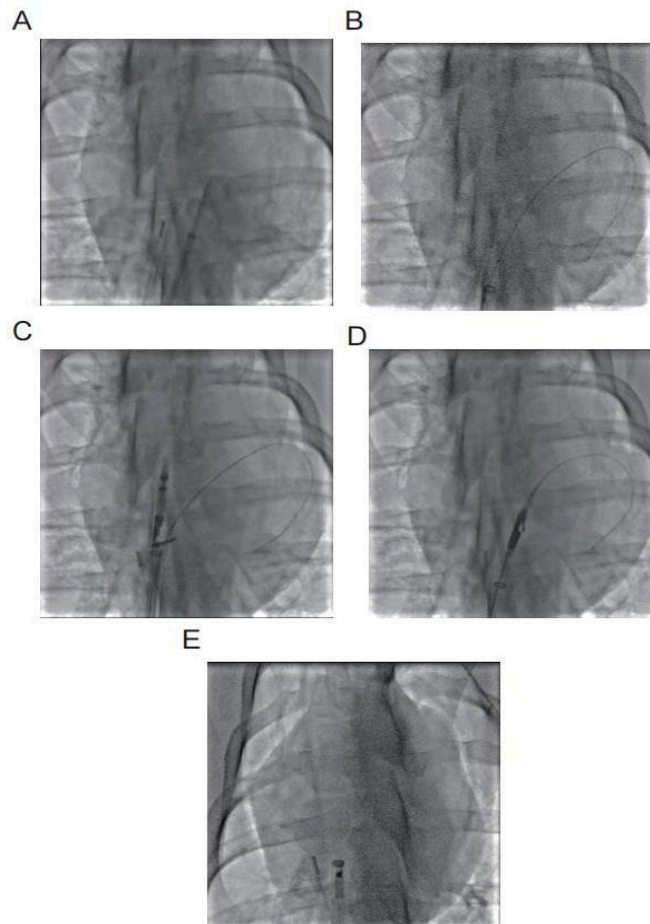


**Figure 2:** (A) Atrial septal puncture into the left atrium; (B) Insert 0.035 guide wire into the left atrium; (C) Secondary septal suture opens the opening arm in the right atrium; (D) Primary septal suture opens the opening arm in the left atrium; (E) Locking device enters the right atrium.

### 3 Result

#### 3.1 Operation

This study involved 13 animals. In two cases, the septum secundum suture device failed to capture the target tissue due to suboptimal puncture positioning (specifically, an excessively low puncture site). These animals were humanely euthanized immediately post-procedure. The remaining 11 animals successfully underwent the implantation of the transcatheter suture system for PFO. Notably, there were no adverse events such as stroke, myocardial infarction, renal failure, pericardial tamponade, or accidental death occurred during the operations.

#### 3.2 Ultrasonic Follow-Up Data

Post-implantation, the locking mechanism remained stable without suture breakage, thrombus formation, or neoplastic changes. The locking device was clearly visualized on ultrasound. Both the atrial septal defect diameter and residual shunt flow velocity decreased significantly over time, with near-complete defect closure observed by 6 months (postoperative ultrasound at immediate, 1, 3 and 6 months respectively, Figs. 3–6). Left ventricular hemodynamics and function remained unaffected.



**Figure 3:** Immediate postoperative ultrasound observation. (A) The locking node is intact, (B) the size of the atrial septal defect is significantly reduced, and (C) there are a few bubbles in the left atrium.

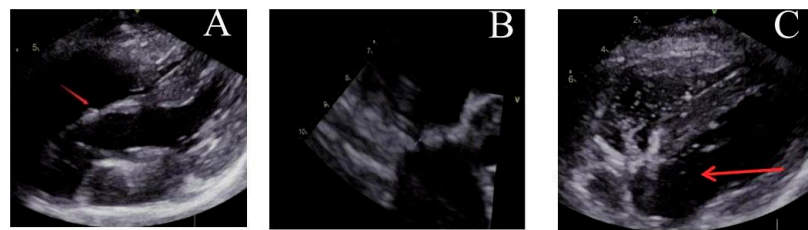


**Figure 4:** Ultrasound observation one month after operation. (A) The locking node is intact, (B) the size of the atrial septal defect further decreases, and (C) there are trace bubbles in the left atrium.

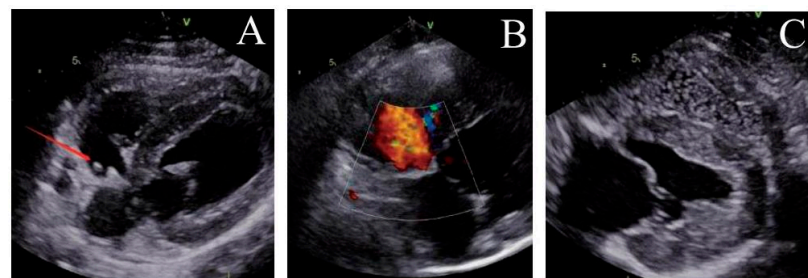


**Figure 5:** Ultrasound observation three months after operation. (A) The locking node is intact, (B) the size of the atrial septal defect further decreases, and (C) there is no bubbles in the left atrium.

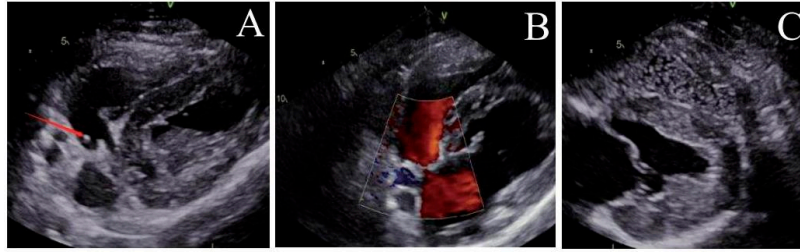


**Figure 6:** Ultrasound observation six months after operation. (A) The locking node is intact, (B) the size of the atrial septal defect further decreases, and (C) there is no bubbles in the left atrium.

### 3.3 Gross Specimen Observation

One month post-operation, the left atrial suture began to show signs of endothelialization (Fig. 7A). Approximately three months after the procedure, endothelialization was observed around the right atrial nail and suture (Fig. 7B). Complete endothelialization of the right atrial suture was evident six months post-operation (Fig. 7C). No evidence of tissue injury, thrombosis, neoplasm, or infection was found at the atrial septal defect site. The defect's orifice was fully healed approximately six months after the procedure. The mitral and tricuspid valves maintained normal structural integrity. There was no displacement or detachment of nails or sutures, no endocardial damage, and no myocardial ischemic infarction detected. Examination of the heart, lungs, liver, spleen, kidneys, and brain revealed no visible infarcts or abnormal lesions (Fig. 8).

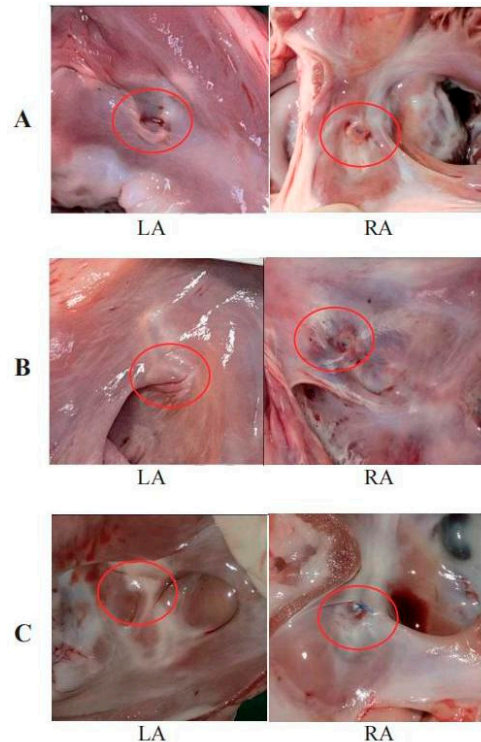


**Figure 7:** (A) Sutures at the left atrial site begin to endothelialize one month after operation. (B) Endothelialization of the lock and suture in the right atrium occurs around 3 months. (C) The defect completely healed after 6 months.

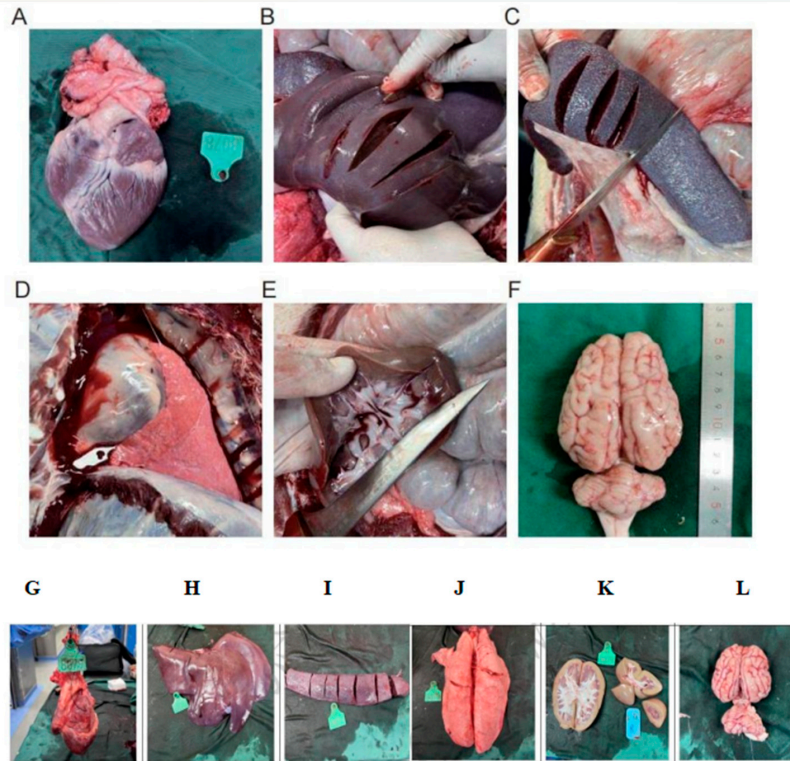


**Figure 8:** Heart (A,G): The adjacent mitral and tricuspid valve structures are normal, there is no damage to the endocardium, and there is no ischemic infarction in the myocardium; No visible infarct lesions were found in the Liver (B,H), Spleen (C,I), Lungs (D,J), Kidneys (E), Brain (F,K,L).

### 3.4 Blood Examination

The average erythrocyte hemoglobin concentration one month after operation was higher compared to pre-operative levels, while other hematological indices showed no significant changes. One month post-operation, all biochemical parameters remained stable. Observations of clinical manifestations and gross anatomical examinations during the animals' care indicated normal liver and kidney functions, with no evidence of hemolysis.

Immediately after the operation, prothrombin time (PT), activated partial thromboplastin time (APTT) and thrombin time (TT) were elevated, while fibrinogen levels were lower compared to pre-operative values. However, one month and three months post-operation, all coagulation indices normalized. This suggests that the immediate post-operative coagulation abnormalities were likely due to the incomplete metabolism of heparin, and that long-term blood coagulation function was not adversely affected by the procedure.

### 3.5 Histopathological Examination

The examination revealed that the head of the implant had a partially organized thrombus, with fibrous connective tissue encapsulation and inflammatory cell infiltration in the polymer materials (Fig. 9). In the liver, false lobules were noted, but no abnormalities were observed in other organs (Fig. 10).

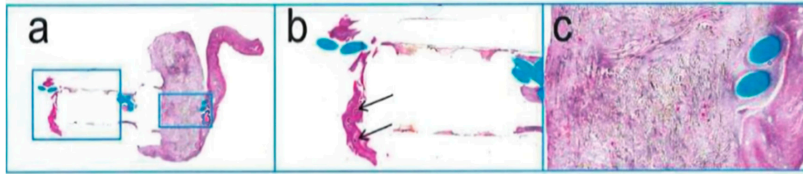


**Figure 9:** H. E. staining of implants; (a): 2.0 $\times$ , (b): 5.0 $\times$ , (c): 10 $\times$ .

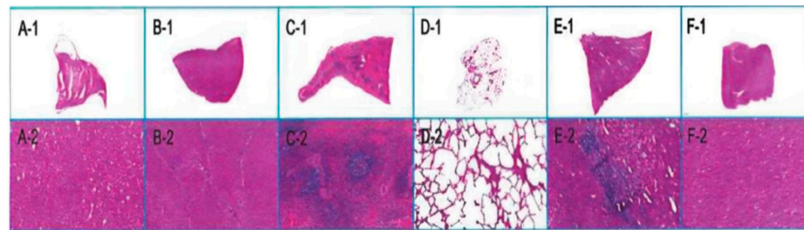


**Figure 10:** Organ pathology map. H. E. Staining; (A-1–F-1): Overall diagram of heart, liver, spleen, lungs, kidneys, and brain; (A-2–F-2): Local maps of heart, liver, spleen, lungs, kidneys, and brain.

#### 4 Discussion

PFO, a prevalent congenital heart disease, is present in approximately 25% of adults [9,10]. Functioning as a conduit between the left and right atrium, PFO can lead to a right-to-left shunt, allowing blood from the right atrium to bypass the pulmonary circulation and directly enter the left atrium. This condition enables certain blood substances to directly transition from venous to arterial circulation, thereby increasing the risk of neurovascular complications [11,12]. Numerous studies [13–16] have confirmed that PFO occlusion can significantly reduce the risk of recurrent strokes in patients with PFO-related stroke. Additionally, migraine symptoms have been reported to either resolve or significantly improving following occlusion therapy. Consequently, the development of PFO devices has become a focal point in the medical industry, with new materials and designs for occluders gradually gaining clinical acceptance.

HaloStitch<sup>®</sup> device represents an innovative advancement in this area, being a new transcatheter suture system specifically designed for PFO based on a suturing concept. Anatomically, most PFOs are slit-like, suggesting that a catheter-based suturing approach may better align with the physiological anatomy of PFOs and offer an effective treatment solution.

##### 4.1 Technical Aspects

The opening and closing arm of the HaloStitch<sup>®</sup> device features a large tissue support, robust tissue capture ability, and an effective thread design that minimize artifacts. This design enhances the clarity of the arm's contour under ultrasound, allowing for precise judgment of its direction and position during the procedure. Additionally, the device's high clamping feedback sensitivity ensures reliable confirmation of tissue capture, thereby improving the success rate of suturing.

The locking mechanism of the HaloStitch<sup>®</sup> is designed for efficiency, capable of locking, cutting, and releasing simultaneously, which simplifies the operation and reduces operation time. Under the guidance of DSA and ultrasound, the operation time of instruments only takes about 15 min. The locking device also includes a feature to prevent thread jamming, eliminating the risk of conveyor jam during cutting.

After undergoing 400 million cycles of dynamic circulation in simulated body conditions (equivalent to 10 years of human implantation), the suture and lock of the HaloStitch<sup>®</sup> demonstrated no signs of detachment, fracture or cracking. This durability contrasts favorably with bioabsorbable occluders, which are prone to dislodgment and difficult removal, thus reducing the potential risk of thrombosis.

While traditional metal occluders have proven effective in various clinical studies, they are associated with adverse reactions and complications such as nickel ion release, intracardiac tissue abrasion, atrial fibrillation, postoperative residual shunt, postoperative arrhythmia, thrombosis and so on [17,18]. The HaloStitch<sup>®</sup> device, employing a polymer implant, is free from metal residues and nickel ion allergies [19,20]. Its small size and lightweight construction minimize cardiac abrasion, promote rapid endothelialization, and reduce the need for prolonged anticoagulation therapy, enhancing safety. Furthermore, its lightweight and compliant nature allows it to move with the heart post-implantation, avoiding undue stress on the atrial septum, thus aligning more closely with physiological anatomy.

In this study, a total of 13 animals were involved, with 11 successfully undergoing suture procedures, translating to a suture success rate of 84.62% using the suture device. Two animals experienced suture failure, attributable to the inappropriate anatomical structure of the foramen ovale and inaccurate ultrasonic positioning during the procedure. The specific reasons for these failures included the following. Firstly, in these cases, the foramen ovale of the animals was anatomically lower, leading to the inability to capture the secondary septum during suturing, resulting in repeated unsuccessful attempts. In addition, the repeated attempts at suturing caused tearing of the entire foramen ovale, making it impossible to complete the procedure. And lastly, real-time ICE with a 10 MHz probe (Philips EPIQ CVx) in bicaval view occasionally failed to definitively visualize the secundum septum-suture arm spatial relationship, while fluoroscopic guidance (Siemens Artis Q) at 15 frames/s and 20° right anterior oblique (RAO) angle provided adequate tracking but limited temporal resolution during rapid cardiac motion phases, resulting in ambiguous tissue capture feedback and hindered dynamic adjustments. Future procedural enhancements include integrating 3D imaging (e.g., Philips X8-2t TEE probe) and pressure-sensing needles (e.g., Baylis Medical VersaCross<sup>®</sup>) for septal alignment and left atrial entry confirmation, optimizing fluoroscopy to 30 frames/sec with dual-plane angiography (RAO 20° + caudal 10°), and preoperative CT/MRI-based anatomical planning to elevate accuracy and reproducibility in challenging PFOs.

Throughout the procedure, the catheter-based PFO stapler system demonstrated the ability to complete the entire instrument implantation effectively under fluoroscopic guidance. The system components, including the septum primum stapler, septum secundum stapler, and the knot locking device, exhibited excellent visibility under X-ray. This feature facilitated the transportation, positioning, suturing, and release of all instruments involved in the procedure. To sum up, the overall operational performance of the transcatheter PFO suture closure system aligns well with clinical demands, showcasing its potential as a viable tool in cardiac interventions.

In this study involving 13 animals, no adverse events related to the instrument were observed during or after the operation. Notably, the surface of the instruments showed no signs of thrombosis, and the implanted sutures and locking nails remained securely in place, without any instances of displacement or detachment. This successful implementation was further evidence by the absence

of complications such as arrhythmia or pericardial tamponade, commonly associated with such procedures. In terms of blood indices and hemodynamics, there were no significant changes observed, indicating a stable postoperative condition. Although a slight increase in the right atrial diameter was noted, likely due to residual blood flow in the early atrial septum, the overall heart structure remained largely unchanged. Furthermore, gross anatomical examination of the animals revealed no abnormalities, with main organs including the heart, liver, spleen, lungs, kidneys, and brain showing no signs of infarct foci and maintaining a normal color and texture.

#### ***4.2 Foramen Ovale Healing and Thrombus Incidence***

The ultrasound follow-up results from our study showed a progressive decrease in the size of the foramen ovale injury over time, culminating in complete healing by six months. Correspondingly, the reflux velocity through the foramen ovale gradually diminished until it ceased entirely. During the operation and postoperative follow-up, no instances of neoplasm or thrombosis was observed under ultrasound. Gross anatomical examination revealed no thrombus formation on the surface of the suture or locking nail. Also, there were no infarcts detected in the core organs of the animals, including the heart, liver, spleen, lungs, kidneys, and brain.

#### ***4.3 Study Limitations***

This study has several limitations that warrant consideration. First of all, as an animal experimental study, it primarily focuses on short-term follow-up results. A longer follow-up duration is necessary to thoroughly evaluate the safety and efficacy of the equipment. Secondly, the defect created by atrial septal puncture in this study more closely resembles an atrial septal defect rather than a PFO [21]. Additionally, the artificially created foramen ovale tends to close spontaneously, which could influence the outcomes and applicability of the results to natural PFO cases.

### **5 Conclusions**

This chronic animal study evaluated the feasibility and safety of a transcatheter PFO suture closure system in swine model. Over the course of this study, observations were made at 30, 90, and 180 days following the implantation of the suture system. The results indicated a lack of adverse events during the extended observation period post-implantation. These findings substantiate the transcatheter PFO suture closure system's feasibility, safety, and biocompatibility within a swine model, demonstrating its potential for effective application in similar medical scenarios.

**Acknowledgement:** We thank all subjects and colleagues for participating in the study.

**Funding Statement:** This work was supported by grants from National High-Level Hospital Clinical Research Funding (2023-GSP-RC-04).

**Author Contributions:** Study conception and design, Haibo Hu and Xiangbing Pan; data collection, Qizong Xie, Qiao Huang and Haiming Wu; analysis and interpretation of results, Haibo Hu, Su Ye, Fengwen Zhang and Jianhua Lv; draft manuscript preparation, Su Ye and Luxi Guan; critical revision of the manuscript for important intellectual content, Dong Luo and Luxi Guan. All authors reviewed the results and approved the final version of the manuscript.

**Availability of Data and Materials:** The datasets generated and/or analyzed during the current study are available from the corresponding author on reasonable request.

**Ethics Approval:** We hereby confirm that our study complies with the Declaration of Helsinki. This study protocol was reviewed and approved by the Ethics Committee of Fuwai Hospital, approval number (NO. 2022-1748).

**Conflicts of Interest:** Qizong Xie, Qiao Huang, and Haiming Wu are employees of Halocinch Medical Technology (Shenzhen) Co., Ltd. The authors declare that they have no financial or personal conflicts of interest that could have influenced the work reported in this manuscript.

## References

1. Teshome MK, Najib K, Nwagbara CC, Akinseye OA, Ibebuogu UN. Patent foramen ovale: a comprehensive review. *Curr Probl Cardiol.* 2020;45(2):100392. [[CrossRef](#)].
2. Alakbarzade V, Keteepe-Arachi T, Karsan N, Ray R, Pereira AC. Patent foramen ovale. *Pract Neurol.* 2020;20(3):225–33. [[CrossRef](#)].
3. Shah AH, Horlick EM, Kass M, Carroll JD, Krasuski RA. The pathophysiology of patent foramen ovale and its related complications. *Am Heart J.* 2024;277:76–92. [[CrossRef](#)].
4. Man H, Xu Y, Zhao Z, Zhang S, Lv R, Chi X, et al. The coexistence of a patent foramen ovale and obstructive sleep apnea may increase the risk of wake-up stroke in young adults. *Technol Health Care.* 2019;27(S1):23–30. [[CrossRef](#)].
5. Shah A, Goerlich CE, Pasrija C, Hirsch J, Fisher S, Odonkor P, et al. Anatomical differences between human and pig hearts and their Relevance for cardiac xenotransplantation surgical technique. *JACC Case Rep.* 2022;4(16):1049–52. [[CrossRef](#)].
6. Thalmann R, Merkel EM, Akra B, Bombien R, Kozlik-Feldmann RG, Schmitz C. Evaluation of hybrid surgical access approaches for pulmonary valve implantation in an acute swine model. *Comp Med.* 2019;69(4):299–307. [[CrossRef](#)].
7. Hořda MK, Hořda J, Koziej M, Piątek K, Klimek-Piotrowska W. Porcine heart interatrial septum anatomy. *Ann Anat.* 2018;217:24–8. [[CrossRef](#)].
8. Lelovas PP, Kostomitsopoulos NG, Xanthos TT. A comparative anatomic and physiologic overview of the porcine heart. *J Am Assoc Lab Anim Sci.* 2014;53(5):432–8.
9. Trumble DR, Magovern JA. Comparison of dog and pig models for testing substernal cardiac compression devices. *Asaio J.* 2004;50(3):188–92. [[CrossRef](#)].
10. Homma S, Messé SR, Rundek T, Sun YP, Franke J, Davidson K, et al. Patent foramen ovale. *Nat Rev Dis Primers.* 2016;2:15086. [[CrossRef](#)].
11. Tateishi Y, Kanamoto T, Yamashita K, Hirayama T, Yoshimura S, Miyazaki T, et al. Biomarkers of cardiac dysfunction as risk factors in cryptogenic stroke. *Cerebrovasc Dis.* 2019;48(3–6):132–9. [[CrossRef](#)].
12. Deng W, McMullin D, Ingleasis-Azuaje I, Locascio JJ, Palacios IF, Buonanno FS, et al. Effect of patent foramen ovale closure after stroke on circulatory biomarkers. *Neurology.* 2021;97(2):e203–14. [[CrossRef](#)].
13. Saver JL, Carroll JD, Thaler DE, Smalling RW, MacDonald LA, Marks DS, et al. Long-term outcomes of patent foramen ovale closure or medical therapy after stroke. *N Engl J Med.* 2017;377(11):1022–32. [[CrossRef](#)].
14. Søndergaard L, Kasner SE, Rhodes JF, Andersen G, Iversen HK, Nielsen-Kudsk JE, et al. Patent foramen ovale closure or antiplatelet therapy for cryptogenic stroke. *N Engl J Med.* 2017;377(11):1033–42. [[CrossRef](#)].
15. Kasner SE, Rhodes JF, Andersen G, Iversen HK, Nielsen-Kudsk JE, Settergren M, et al. Five-year outcomes of PFO closure or antiplatelet therapy for cryptogenic stroke. *N Engl J Med.* 2021;384(10):970–1. [[CrossRef](#)].
16. Meier B, Kalesan B, Mattle HP, Khattab AA, Hildick-Smith D, Dudek D, et al. Percutaneous closure of patent foramen ovale in cryptogenic embolism. *N Engl J Med.* 2013;368(12):1083–91. [[CrossRef](#)].

17. Tang B, Su F, Sun X, Wu Q, Xing Q, Li S. Recent development of transcatheter closure of atrial septal defect and patent foramen ovale with occluders. *J Biomed Mater Res B Appl Biomater.* 2018;106(1):433–43. [[CrossRef](#)].
18. Happel CM, Laser KT, Sigler M, Kececioglu D, Sandica E, Haas NA. Single center experience: implantation failures, early, and late complications after implantation of a partially biodegradable ASD/PFO-device (BioStar<sup>®</sup>). *Catheter Cardiovasc Interv.* 2015;85(6):990–7. [[CrossRef](#)].
19. Li B, Xie Z, Wang Q, Chen X, Liu Q, Wang W, et al. Biodegradable polymeric occluder for closure of atrial septal defect with interventional treatment of cardiovascular disease. *Biomaterials.* 2021;274:120851. [[CrossRef](#)].
20. Xu Q, Fa H, Yang P, Wang Q, Xing Q. Progress of biodegradable polymer application in cardiac occluders. *J Biomed Mater Res B Appl Biomater.* 2024;112(1):e35351. [[CrossRef](#)].
21. Buecker A, Spuentrup E, Grabitz R, Freudenthal F, Muehler EG, Schaeffter T, et al. Magnetic resonance-guided placement of atrial septal closure device in animal model of patent foramen ovale. *Circulation.* 2002;106(4):511–5. [[CrossRef](#)].